Electronic Supplementary Material (ESI) for Physical Chemistry Chemical Physics.

Photoinduced excitation and charge transfer processes of organic dyes with siloxane anchoring groups: a combined spectroscopic and computational study

Supporting Information

Stationary absorption spectra of the remaining compounds

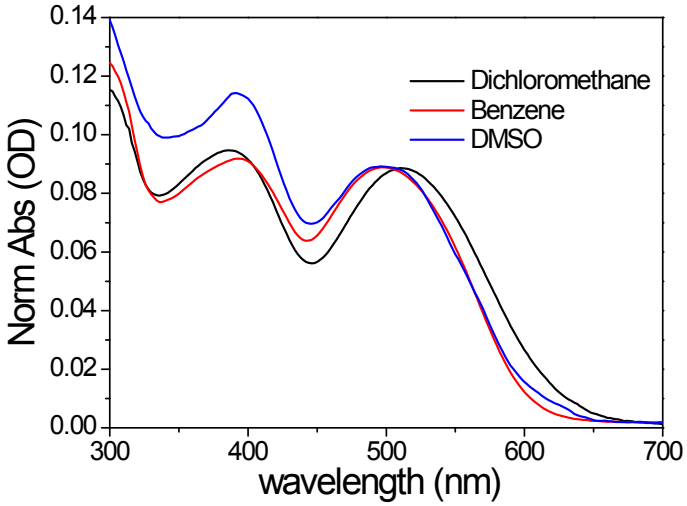

Figure S1: Absorption spectra of **MM62** in dichloromethane, acetonitrile and benzene

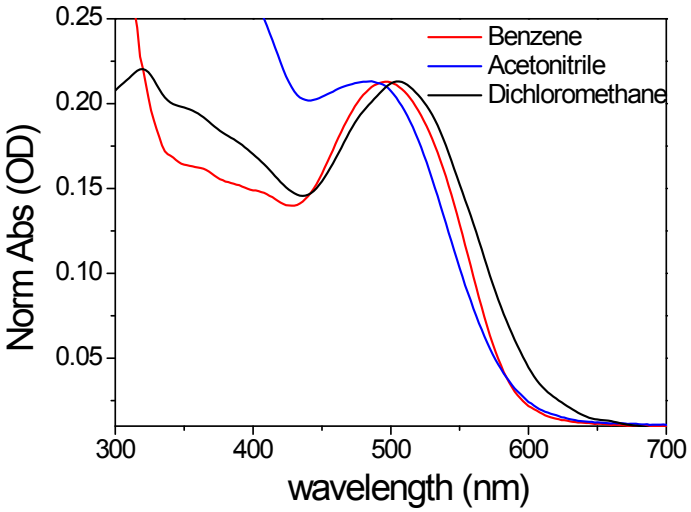

Figure S2: Absorption spectra of **MB56** in dichloromethane, acetonitrile and benzene

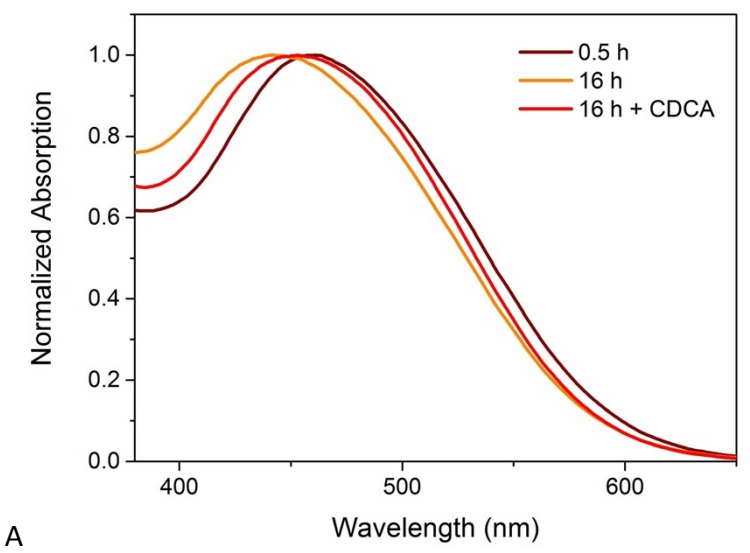

A

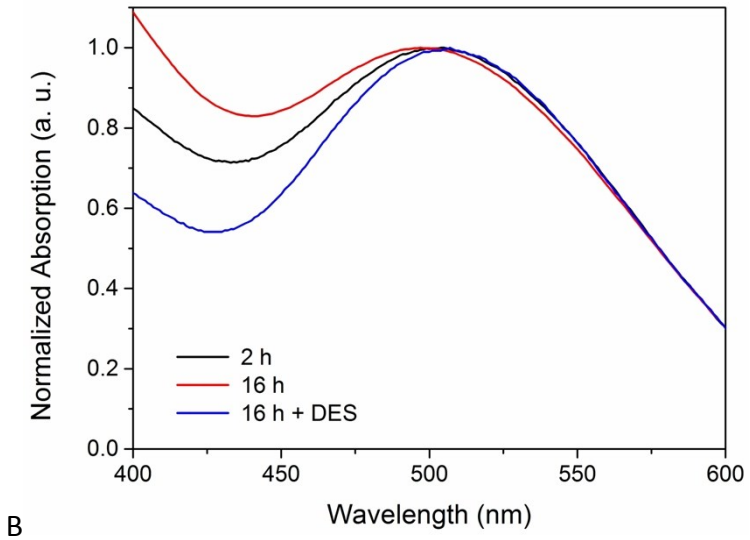

B

Figure S3: Effect of the staining time and of the addition of co-adsorbent on the absorption spectrum of dyes on a TiO_2 film. Panel A) reports the normalized spectra of **DF15** in the presence of CDCA (chenodeoxycholic acid) and as a function of the staining time; Panel B) reports the normalized spectra of **MM62** in the presence of DES (dodecyltriethoxysilane) and as a function of the staining time.

Fluorescence spectra

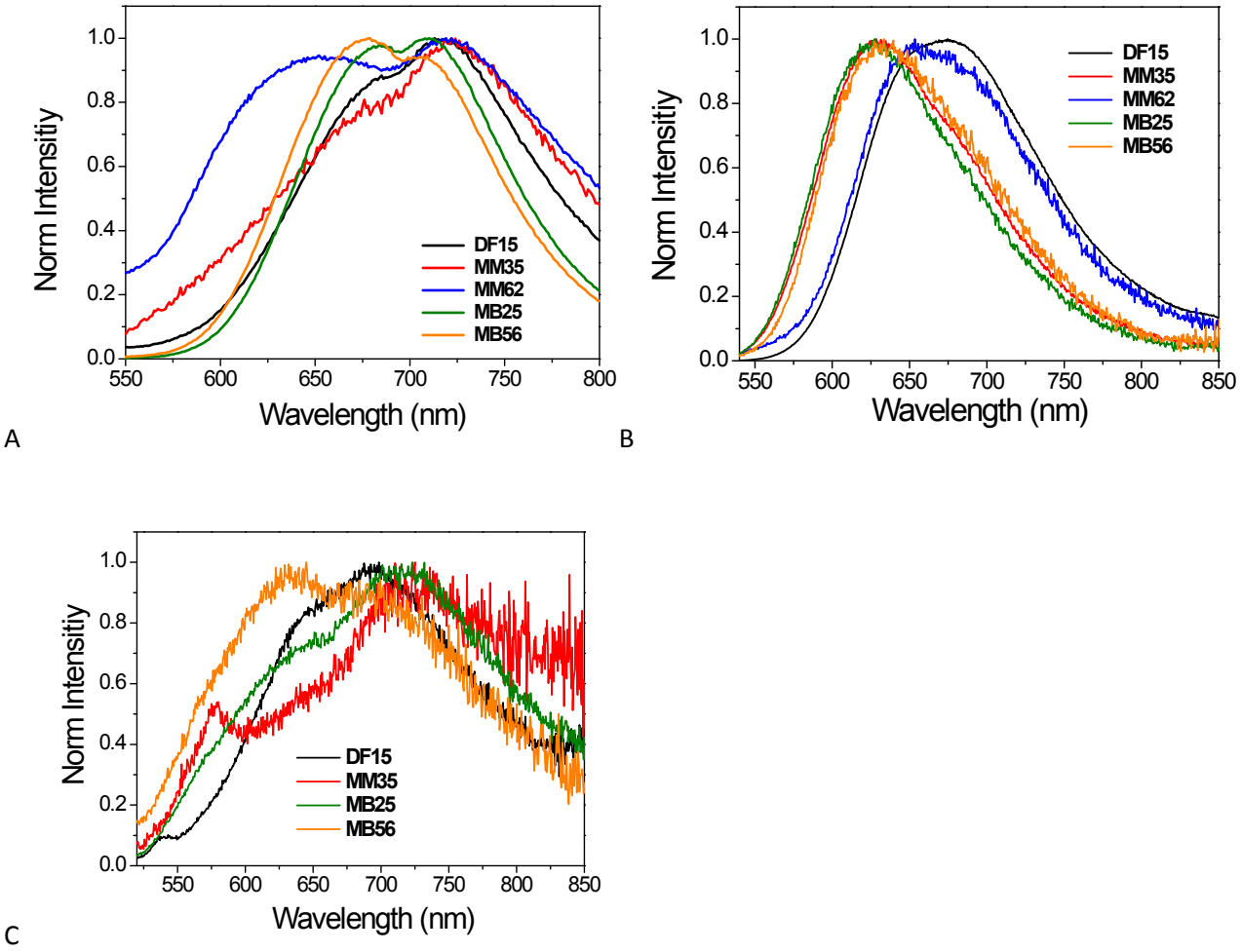

Figure S4: Normalized fluorescence spectra of all the analyzed dyes in A) dichloromethane; B) benzene; C) acetonitrile

Additional Transient Absorption Measurements

DF15 in different solvents

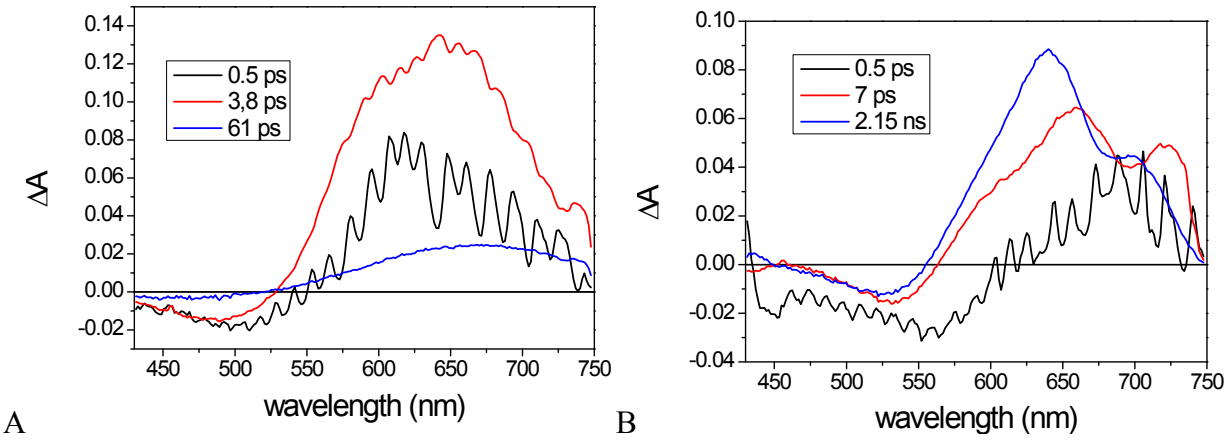

Figure S5: EADS obtained by the global analysis of transient data recorded for **DF15** in A) acetonitrile; B) benzene.

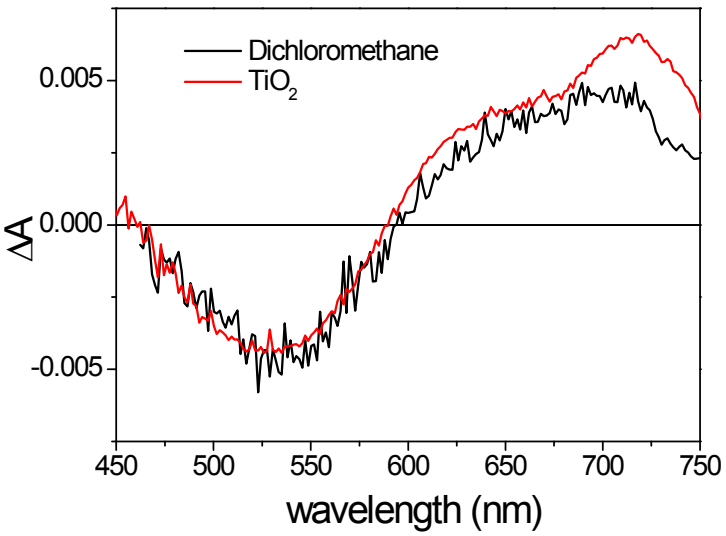

Figure S6: Comparison between the last EADS measured for **DF15** in dichloromethane and on the TiO_2 surface.

MM35 in different solvents

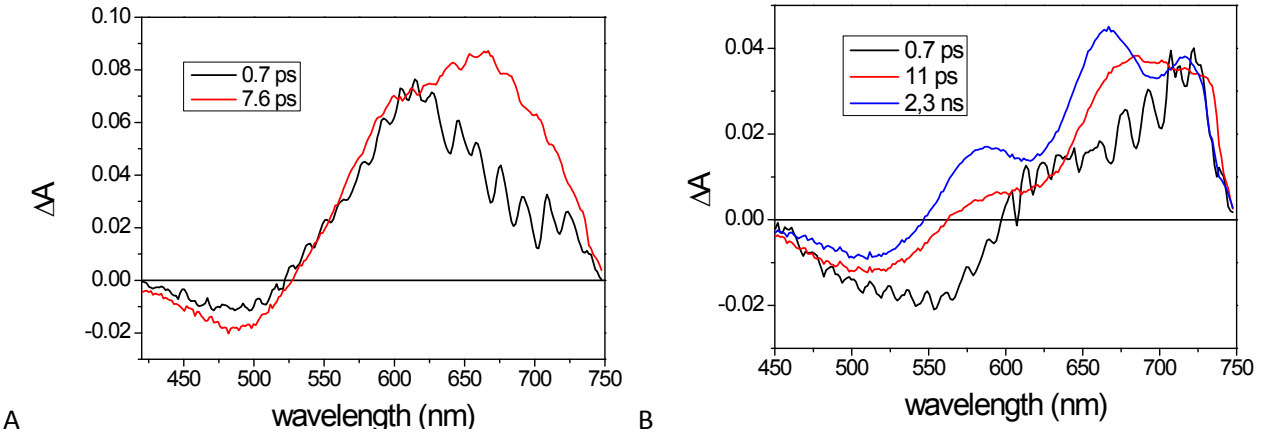

Figure S7: EADS obtained by the global analysis of transient data recorded for **MM35** in A) acetonitrile; B) benzene.

MM62 in different solvents

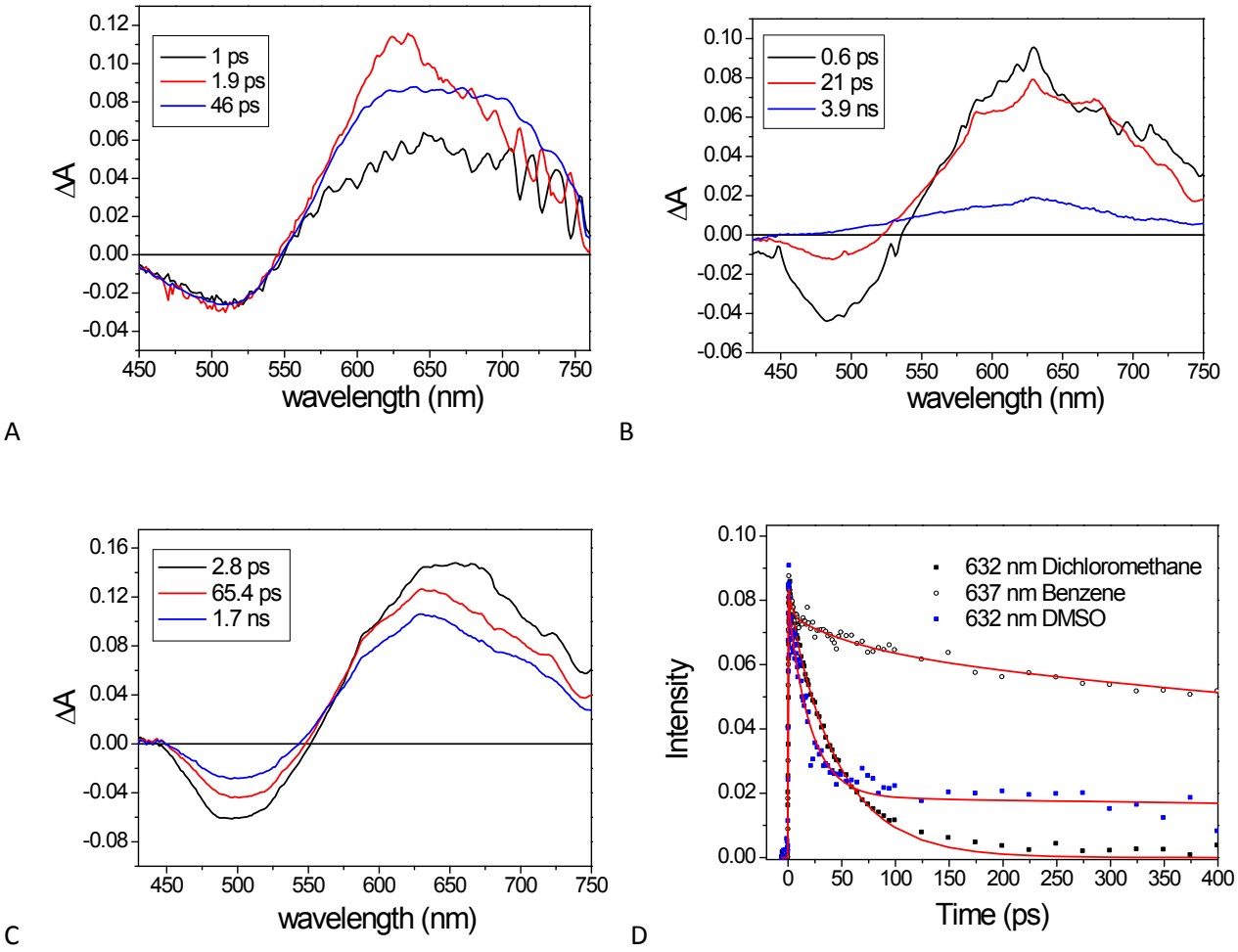

Figure S8: EADS obtained by the global analysis of transient data recorded for **MM62** in A) dichloromethane; B) DMSO; C) Benzene. DMSO was used as polar solvent in the case of **MM62** because of the very low solubility of the latter in acetonitrile. Panel D) reports the kinetic trace at 632-637 nm registered in the different solvents (scattered points) together with the fit resulting from global analysis (red line).

MB25 in different solvents

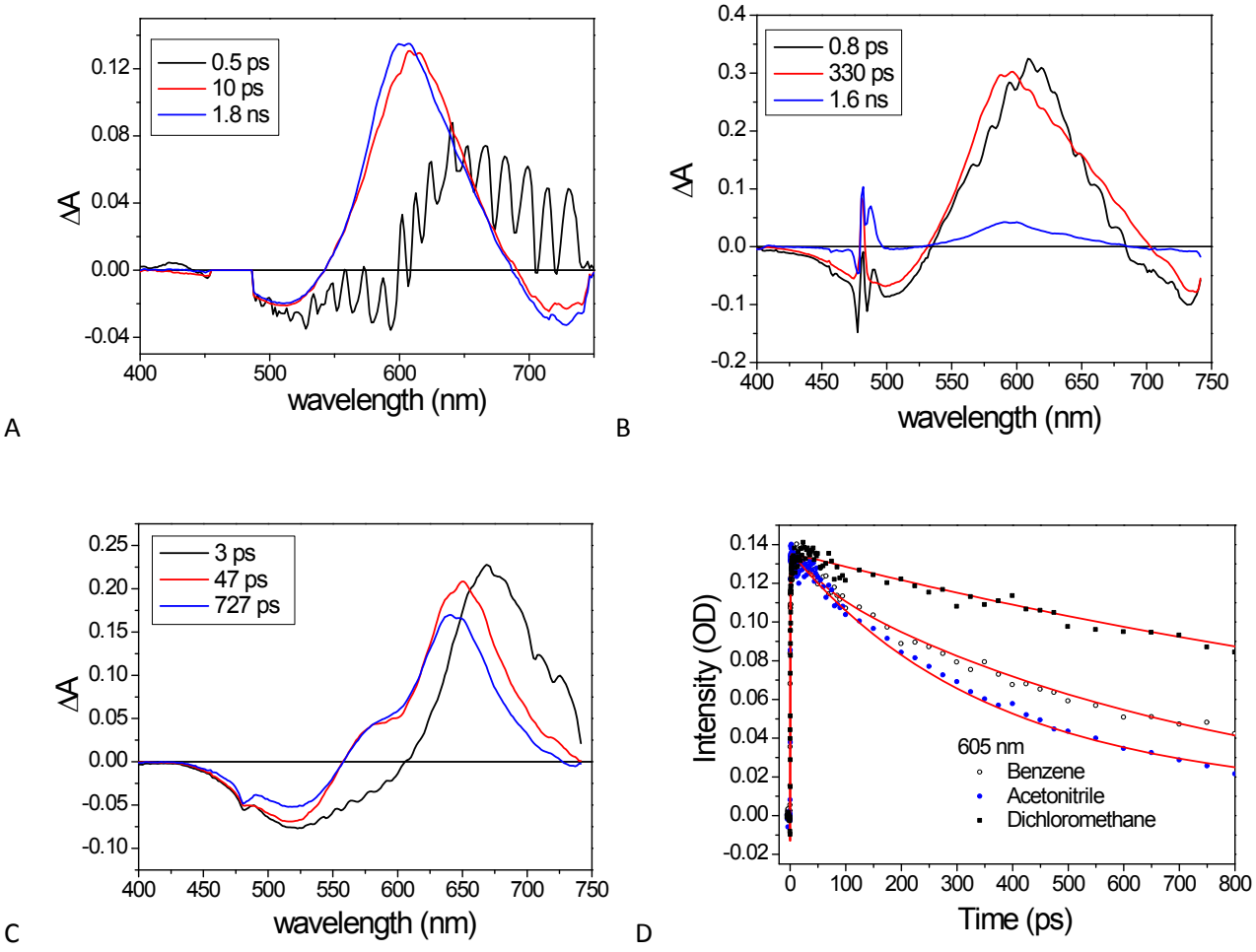

Figure S9: EADS obtained by the global analysis of transient data recorded for **MM25** in A) dichloromethane; B) acetonitrile; C) benzene. Panel D) reports the kinetic traces at 605 nm registered in the three solvents (scattered points) together with the fit resulting from global analysis (red line).

MB56 in different solvents

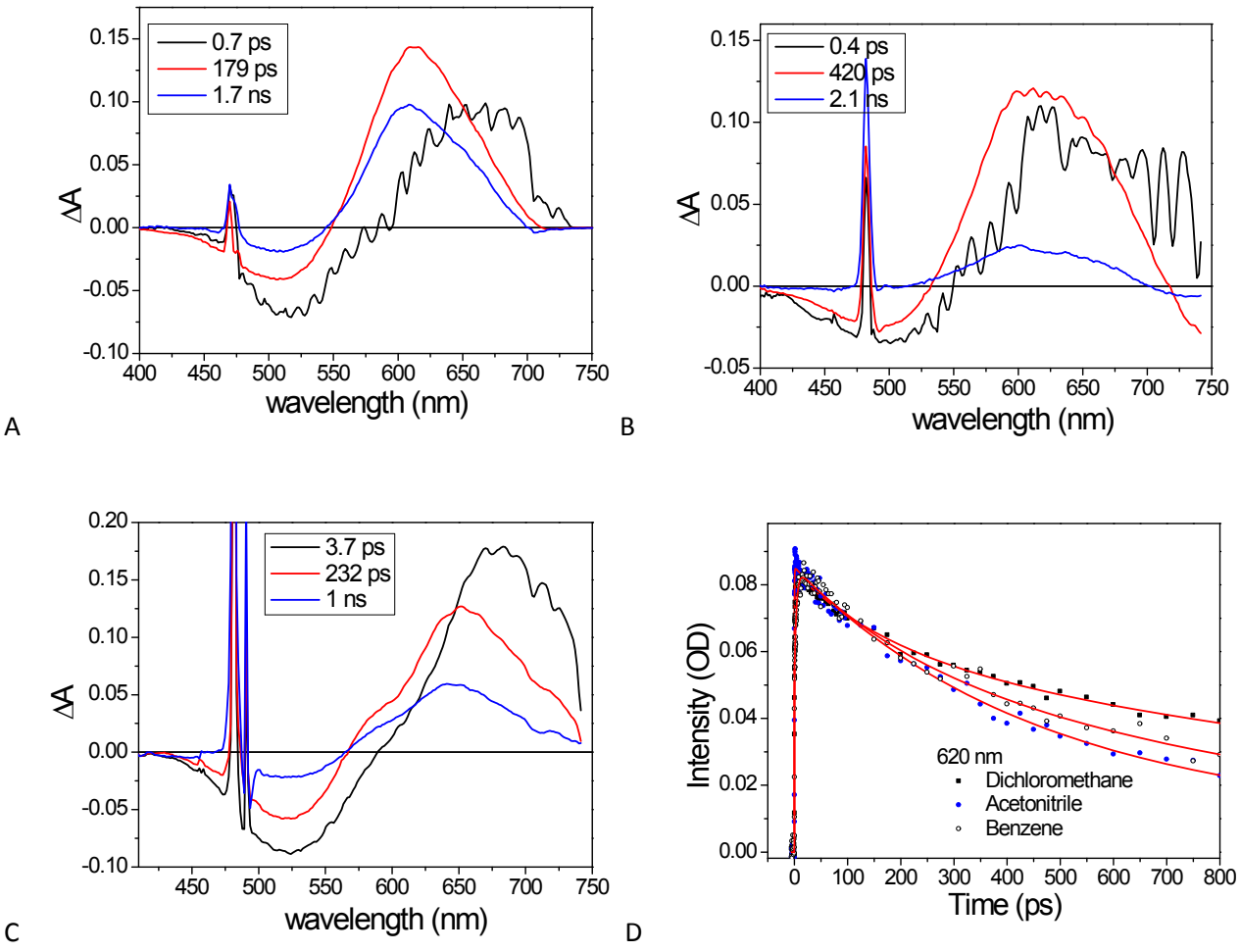

Figure S10: EADS obtained by the global analysis of transient data recorded for **MM56** in A) dichloromethane; B) acetonitrile; C) benzene. Panel D) reports the kinetic traces at 620 nm registered in the three solvents (scattered points) together with the fit resulting from global analysis (red line).

Additional computational results

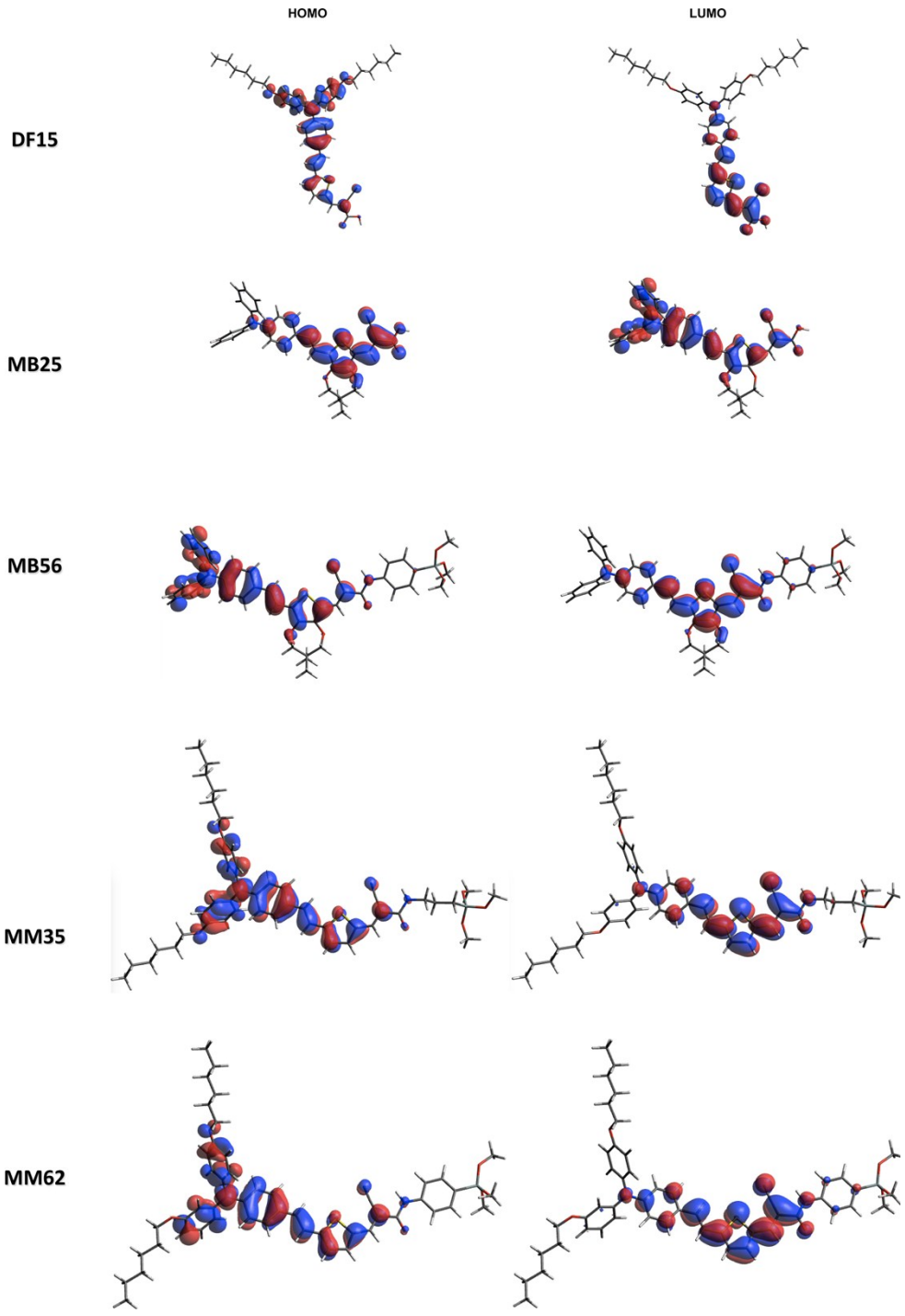

Figure S11: Wave function plots of the HOMO and LUMO orbitals of compounds **DF15, MB25, MB56, MM35** and **MM62**. Adapted from reference (M. Bessi et al., "Synthesis of Silatrane-Containing Organic Sensitizers as Precursors for Silyloxyl Anchoring Group in Dye Sensitized Solar Cells", Synthesis, 2017, manuscript accepted for publication).

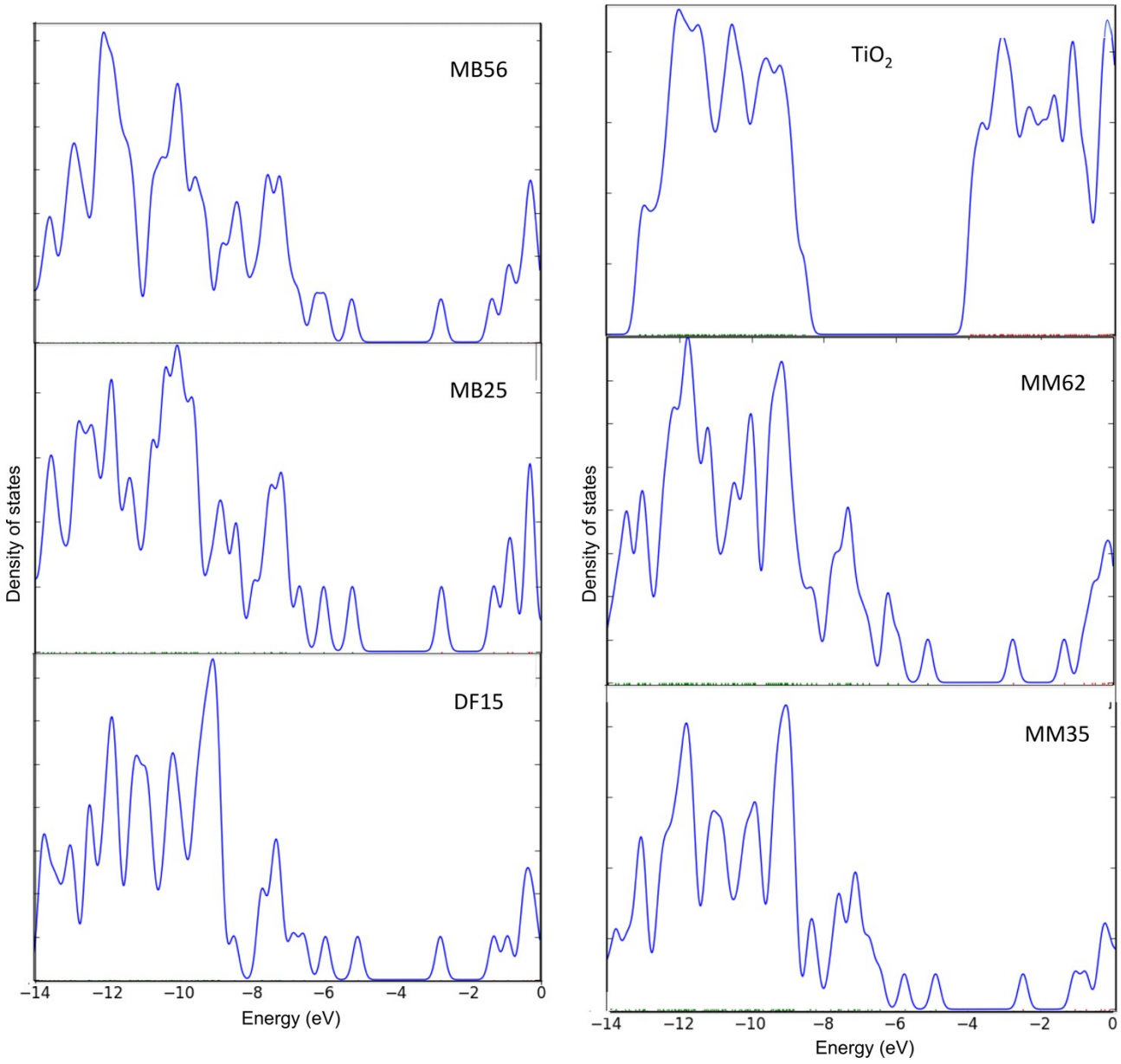

Figure S12: TDOS of isolated **DF15, MB25, MB56, MM35** and **MM62** dyes and bare $(TiO_2)_{16}$.

Table S1

TD-DFT (CAM-B3LYP/6-31G* and, in brackets, MPW1K/6-31G*) computed absorption maxima (λ^a_{max}), energy (E_{exc}), oscillator strengths (f) and composition in terms of molecular orbitals for the lowest singlet-singlet excitation of the deprotonated form of DF15 (DF15-deprot[a]) and for the S_2, S_3 and S_4 states (which are shown along with the lowest singlet-singlet excitation, S_1) of MB25 and MB56 in CH_2Cl_2, C_6H_6 and CH_3CN:

Dye		λ^a_{max} (nm)	E_{exc} (eV)	f	Transitions
DF15-deprot	CH_2Cl_2	420 (434)	2.95 (2.83)	1.561 (1.509)	H->L 74% (86%)
	C_6H_6	411 (423)	3.01 (2.93)	1.600 (1.630)	H->L 86% (92%)
	CH_3CN	423 (444)	2.93 (2.80)	1.530 (1.447)	H->L 73% (86%)
MB25	CH_2Cl_2	477 (497) (S_1)	2.60 (2.49) (S_1)	1.505 (1.494) (S_1)	H->L 80% (91%) (S_1)
		338 (356) (S_2)	3.67 (3.48) (S_2)	0.178 (0.125) (S_2)	H-1->L 71% (89%) (S_2)
		322 (320) (S_3)	3.85 (3.87) (S_3)	0.103 (0.101) (S_3)	H-2-> L 86% (86%) (S_3)
		290 (301) (S_4)	4.28 (4.12) (S_4)	0.278 (0.381) (S_4)	H->L+1 69% (87%) (S_4)
	C_6H_6	475 (493) (S_1)	2.61 (2.51) (S_1)	1.519 (1.518) (S_1)	H->L 80% (90 %)(S_1)
		336 (353) (S_2)	3.69 (3.51) (S_2)	0.196 (0.122) (S_2)	H-1->L 70% (89%) (S_2)
		319 (317) (S_3)	3.89 (3.91) (S_3)	0.099 (0.090) (S_3)	H-2 ->L 85% (85%)(S_3)
		289 (300) (S_4)	4.29 (4.13) (S_4)	0.259 (0.391) (S_4)	H ->L+1 66% (86%)(S_4)
	CH_3CN	476 (496) (S_1)	2.61 (2.50) (S_1)	1.491 (1.475) (S_1)	H->L 80% (91%)(S_1)
		338 (356) (S_2)	3.67 (3.48) (S_2)	0.168 (0.127) (S_2)	H-1->L 71% (90%) (S_2)
		323 (321) (S_3)	3.84 (3.86) (S_3)	0.101 (0.101) (S_3)	H-2 ->L 86% (87%)(S_3)
		290 (301) (S_4)	4.28 (4.12) (S_4)	0.279 (0.372) (S_4)	H ->L+1 70% (87%)(S_4)
MB56	CH_2Cl_2	479 (499) (S_1)	2.59 (2.48) (S_1)	1.733 (1.721) (S_1)	H->L 80% (90%) (S_1)
		339 (358) (S_2)	3.66 (3.47) (S_2)	0.271 (0.230) (S_2)	H-1->L 70% (89%) (S_2)
		320 (319) (S_3)	3.88 (3.89) (S_3)	0.103 (0.122) (S_3)	H-3->L 82% (76%)(S_3)
		291 (302[§])(S_4)	4.27 (4.10[§])(S_4)	0.286 (0.378[§])(S_4)	H ->L+1 62% (80%[§])(S_4)

	C_6H_6	477 (495) (S_1)	2.60 (2.50) (S_1)	1.741 (1.741) (S_1)	H->L 80% (90%) (S_1)
		338 (356) (S_2)	3.67 (3.49) (S_2)	0.285 (0.231) (S_2)	H-1->L 70% (89%) (S_2)
		317 (316) (S_3)	3.91 (3.92) (S_3)	0.101 (0.131) (S_3)	H-3->L 82% (58%)(S_3)
		289[&] (302 [§]) (S_5)	4.28[&] (4.11[§])(S_5)	0.236[&] (0.394[§])(S_5)	H ->L+1 61%[&] (81%[§])(S_5)
	CH_3CN	478 (498) (S_1)	2.60 (2.49) (S_1)	1.728 (1.710) (S_1)	H->L 80% (90%) (S_1)
		338 (358) (S_2)	3.66 (3.47) (S_2)	0.263 (0.231) (S_2)	H-1->L 70% (89%) (S_2)
		320 (319) (S_3)	3.87 (3.89) (S_3)	0.100 (0.119) (S_3)	H-3->L 82% (77%)(S_3)
		290 (302[§])(S_4)	4.27 (4.10[§])(S_4)	0.280 (0.364[§])(S_4)	H ->L+1 65% (86%[§])(S_4)

[a]**DF15**-deprot corresponds to the **DF15** molecule in which the cyanoacrylic acid anchoring group is deprotonated; [§]These values correspond to the computed S_5 state (the computed S_4 state has a negligible value for the oscillator strength); [&]These values correspond to the computed S_5 state (the computed S_4 state has a lower value for the oscillator strength).

Table S2

TD-DFT (CAM-B3LYP/6-311+G(2d,p)) computed absorption maxima (λ^a_{max}), excitation energy (E_{exc}), oscillator strengths (f) and composition in terms of molecular orbitals for the lowest singlet-singlet excitation of DF15 and of the deprotonated form of DF15 (DF15-deprot[a]) in CH_2Cl_2, C_6H_6 and CH_3CN:

Dye		λ^a_{max} (nm)	E_{exc} (eV)	f	Transition H→L
DF15	**CH_2Cl_2**	508.97	2.4360	1.5944	77%
	C_6H_6	506.64	2.4472	1.6050	77%
	CH_3CN	506.75	2.4467	1.5829	77%
DF15-deprot[a]	**CH_2Cl_2**	439.42	2.8215	1.5348	73%
	C_6H_6	428.20	2.8955	1.5707	83%
	CH_3CN	443.24	2.7972	1.5065	72%

[a]**DF15**-deprot corresponds to the **DF15** molecule in which the cyanoacrylic acid anchoring group is deprotonated.

Table S3

***In vacuo* FMOs energies of DF15, MB25, MB56, MM35 and MM62 at the B3LYP/6-31G* level:**

Dye	Energy (eV)				
	HOMO-1	HOMO	LUMO	LUMO+1	Δ(H-L)
DF15	-5.68649164	-4.79720348	-2.52962752	-1.02344332	-2.26757596
MB25	-5.76268524	-4.96836696	-2.5198312	-1.04303596	-2.44853576
MB56	-5.70145824	-4.96591788	-2.51357244	-1.07106432	-2.45234544
MM35	-5.56784732	-4.70794812	-2.32771448	-0.87867548	-2.38023364
MM62	-5.70581216	-4.88945216	-2,56037708	-1.10643992	-2.32907508

Table S4

FMOs energies of DF15, MB25, MB56, MM35 and MM62 on TiO_2 and *in vacuo* at the B3LYP/6-311G(d,p) level (the standard LANL2DZ basis set was used for the Ti atom):

Dye		Energy (eV)				
		HOMO	LUMO	LUMO+8	LUMO+12	Δ(H-L)
DF15	TiO_2	-5.44348848	-3.53864848			-1.90484000
	in vacuo	-5.03802968	-2.74922836			-2.28880132
MB25	TiO_2	-5.49709612	-3.48504084			-2.01205528
	in vacuo	-5.20728832	-2.74460232			-2.46268600
MB56	TiO_2	-5.24674572	-3.57293560	-3.02651864		-1.67381012
	in vacuo	-5.20021320	-2.73371752			-2.46649568
MM35	TiO_2	-5.01898128	-3.62518264		-2.93889600	-1.39379864
	in vacuo	-4.94686948	-2.54268928			-2.4041802
MM62	TiO_2	-5.16483760	-3.57266348	-3.02352532		-1.59217412
	in vacuo	-5.12483596	-2.77671248			-2.34812348

References

1. Kelly, S. M.; Lipshutz, B. H., *Org. Lett.* **2014**, *16*, 98-101.